

**POLITECNICO
MILANO 1863**

**Optimal Trajectory Planning for a Tractor
Maneuver in a Field**

**Constrained and Numerical Optimization
for Estimation and Control**

Academic Year 2023/2024

Group members

Lorenzo Petulicchio 10639923
Davide Vedani 10571861

Contents

Introduction	3
Notation	4
1. Problem statement	6
2. System description	7
2.1. Assumptions	7
2.2. Tractor model	8
2.3. Tractor and implement model	9
3. Problem Abstraction	11
3.1. Numerical Integration	11
3.2. Optimization problem	13
3.3. Cost function	14
3.4. Constraints	15
3.5. Tractor and implement variations	16
4. Optimization procedure	18
4.1. Downsampling input variables	18
4.2. Possible maneuvers	18
4.3. Initial condition	19
4.4. Implemented optimization problem	20
4.5. Optimization tools	21
5. Results	22
5.1. Tractor only	22
5.2. Tractor and implement	27
6. Conclusions	31
Bibliography	32

Introduction

The agriculture industry is facing unprecedented challenges, with rising input costs, the growing impact of climate and a significant labor shortage, a challenge that threatens the sustainability and productivity of farming operations worldwide. In particular, in both the European Union and the United States, the agricultural workforce is aging, and the influx of younger workers is insufficient to replace those who are retiring or leaving the field.

In the European Union, the situation is particularly concerning. As of 2020, over two-thirds of the EU's 9.1 million farm managers were male, and more than half were at least 55 years old. Young farmers, defined as those under 40, make up a mere 11.9% of the total. This aging demographic, coupled with a declining number of farms, has led to a significant reduction in the agricultural workforce. [1]

The United States is facing similar challenges. The average age of farmworkers, particularly among foreign-born laborers, has been steadily increasing. Between 2006 and 2021, the average age of immigrant farmworkers rose by seven years, highlighting the lack of younger workers entering the field. This aging workforce, combined with a reduced flow of younger immigrants into agriculture, is putting additional pressure on the industry. [2]

In response to these pressures, the adoption of innovative solutions has become crucial for the survival and growth of the agriculture industry. Automation and smart agriculture technologies offer promising avenues for mitigating the adverse effects of these challenges. From semi-automated systems like assisted steering to fully autonomous technologies such as weeding robots and precision agriculture tools, these advancements are enabling farmers to enhance efficiency, reduce input costs, and optimize their operations.

This project draws inspiration from existing research in agricultural automation, particularly focusing on the maneuver that a tractor must frequently perform in the field to ensure rows remain parallel when transitioning from one row to the next [3]. Our work aims to optimize execution times, improve the robustness and adaptability for different headland configurations, and select the most effective maneuvering strategies.

Notation

Notation	Meaning	Unit
<i>Tractor model variables</i>		
x_t	X-coordinate of the tractor's COG	m
y_t	Y-coordinate of the tractor's COG	m
ψ_t	Heading angle of tractor	rad
v_t	Velocity of tractor COG	m/s
a_t	Acceleration of tractor COG - <i>input variable</i>	m/s ²
δ_t	Steering angle of tractor - <i>input variable</i>	rad
<i>Implement model variables</i>		
x_i	X-coordinate of the implement's COG	m
y_i	Y-coordinate of the implement's COG	m
ψ_i	Heading angle of implement	rad
v_i	Velocity of implement COG	m/s
δ_i	Relative angle between heading of tractor and implement	rad
<i>Optimization problem variables</i>		
t	Discrete Time	-
T_s	Simulation sampling time	s
γ	Weighting parameter for the two terms of the cost function	-
p	Weighting vector for the error of the final states	-
c_{vel}	Parameter to control the speed constraint	-
U_0	Initial sequence of control variable	-
z_0	Initial value of the states	-
z_f	Desired final value of the states	-

Table 1: Table of variables in equations

Notation	Meaning	Value	Unit
<i>Models parameters</i>			
L_t	Wheelbase of the tractor	3	m
L_i	Wheelbase of the implement	2	m
L_h	Distance between tractor COG and towing point	0	m
<i>Headland configuration parameters</i>			
d	Distance between rows	4	m
<i>Saturation limits and tolerances</i>			
v_{\min}	Minimum allowed speed	4.17	m/s
v_{\max}	Maximum allowed speed	-4.17	m/s
a_{\min}	Minimum allowed acceleration	1	m/s^2
a_{\max}	Maximum allowed acceleration	1	m/s^2
δ_{\min}	Minimum allowed steering angle	$\frac{\pi}{6}$	rad
δ_{\max}	Maximum allowed steering angle	$\frac{\pi}{6}$	rad
$\delta_{i_{\max}}$	Maximum allowed relative heading angle between tractor and implement	$\frac{5\pi}{12}$	rad
l_b	Lower bound vector of input saturation	*	-
u_b	Upper bound vector of input saturation	*	-
tol_f	Vector of tolerances for the error of the final states	*	-
<i>Optimization problem parameters</i>			
N_s	Simulation steps	75	-
N_p	Input vector size	38	-

Table 2: Table of parameters

1. Problem statement

As stated in the introduction, this work focuses on a specific maneuver that agricultural machinery needs to perform multiple times. Since efficient use of the terrain is crucial in this field, maintaining rows parallel and equally spaced according to the row width, d , is one of the most important features. To achieve this the tractor needs to arrive at the final point, the one from which the row is then worked, with a specific orientation. The operational area where the tractor must perform the maneuver before entering the next row, is called *headland*. The final pose of the tractor is heading parallel with respect starting point but in opposite direction. A schematic representation is provided in Figure 1, depicting an ideal case without considering the real dynamics of the tractor.

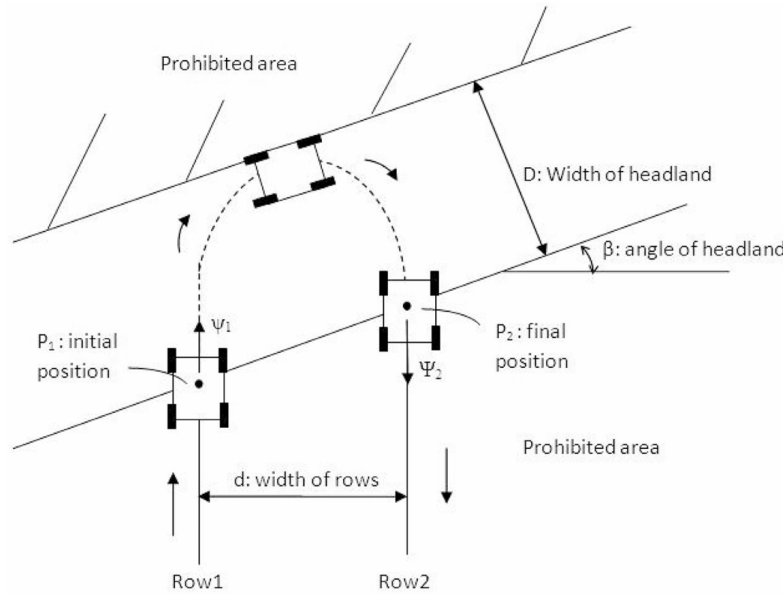


Figure 1: Headland maneuver schematic.¹

Figure 2 shows a realistic example of a headland, taken from a satellite image of a field in southern Milan, Italy. The green area defines the operational space, typically constrained by a prohibited area and the actual field, both of which must be avoided during the maneuvering phase and are here colored in red. The objective of this work is to develop an algorithm to compute the optimal trajectory for executing the described maneuver.



Figure 2: Headland operational area example.²

¹Image taken from [3]

²Image taken from Google Maps

2. System description

The optimization approach developed in this project is designed to address a range of scenarios involving various headland configurations and maneuvering operations within a cluttered operational space. The working phase of the tractor's trajectory is straightforward, following a fixed path along the rows. However, the maneuvering phase presents more interesting challenges, particularly in optimizing execution time or minimizing traveled distance. These challenges create opportunities for optimization, which is the focus of this project. Here, are detailed the models and assumptions used to solve the problem outlined in previous sections.

2.1. Assumptions

The mathematical model developed to approach the optimization problem has been obtained under the following assumptions.

- The tractor is assumed to perform the maneuver at low and slow varying velocity, an hypothesis that is consistent with chosen mathematical model, described in Section 2.2.
- The initial and final velocities of the tractor are equal and non-zero, as the maneuver begins with the tractor exiting a row and concludes at the point where it must continue along the next row.
- L_h , the length of the hook connecting the tractor and the implement, is considered negligible and set equal to zero since it is small with respect to the wheelbase of the two vehicles.
- The headland is free of obstacles and could be well described by two lines in the 2D space.
- The linear approximations of the headland limits, specified in Section 3, take into account the physical dimensions of the tractor and implement. This implies that only the center of gravity (COG) of the two vehicles must satisfy those constraints.
- The distance between rows, d , is assumed to be known a priori, as it directly depends on the operational width of the attached implement.
- When the implement is towed by the tractor, the tractor itself may enter the prohibited area of the field, as it is the position of the attached implement that needs to be controlled to keep the rows parallel. Moreover, for the same reasoning, the initial position of the tractor, in this case, is already in the headland.

2.2. Tractor model

The first step to find a correct solution to this problem is to find a mathematical model of the tractor that accurately describes the motion of the vehicle. This model must be accurate in this description, but should also not be overly complex.

The vehicle which has been considered is a front wheel steering tractor, as shown in Figure 3. It can be assumed without making significant errors that the center of mass lies at the center of the rear axle, since in these kind of vehicles most of the mass is concentrated in the rear part

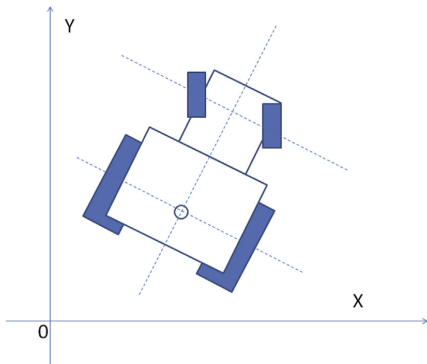


Figure 3: Tractor representation³

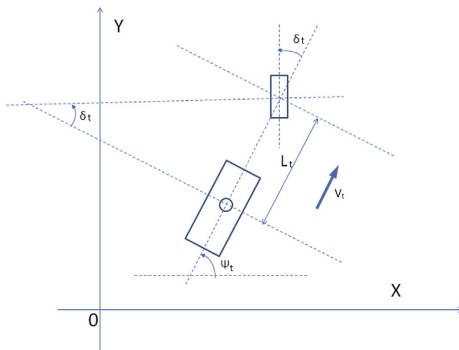


Figure 4: Kinematic bicycle model of tractor³

One possible choice for the model could be to use a dynamical bicycle model. But this is a quite complex model that uses lots of nonlinear dynamic equations, also due to the fact that it takes into account the slip of tires and the forces generated between tires and soil. The result is a complex model that describes very well the dynamic of the system, but it is overly complex for simulation of the studied vehicle.

To overcome this complexity, a well-established method is to use the kinematic bicycle model. The big advantage with respect to the dynamical one is that in this model the tire dynamic is neglected. This means that slip and contact force of tires are not considered and the wheels are assumed to be traveling in the direction they are facing. These simplifications can be done accordingly to the assumptions on the low and slowly varying speed.

A graphical representation of this model is given in Figure 4. As can be seen from this image, the kinematic bicycle model describes the behavior of the vehicle with respect to a global reference frame. In this work, the origin of this reference frame is set in the point where the maneuver starts, that is the point where the tractor exits from the field. The Y axis is aligned with the longitudinal axis of the vehicle and the X axis is perpendicular to it on the right side.

The states of the tractor model are four, where the subscript t refers to *tractor*:

- The position of the center of gravity on the X and Y axis, labeled as x_t and y_t
- The heading angle, that is the angle between the longitudinal axis of the vehicle and the X axis of the global reference frame, labeled as ψ_t
- The speed of the center of gravity, labeled as v_t

Then the complete state vector is

³Images taken from [3]

$$z_t = \begin{bmatrix} x_t \\ y_t \\ \psi_t \\ v_t \end{bmatrix} \quad (1)$$

Since slip or force on tires are neglected, the evolution of the system's states in continuous time can be described using geometrical relations only, as follows:

$$\begin{cases} \dot{x}_t = v_t \cos(\psi_t) \\ \dot{y}_t = v_t \sin(\psi_t) \\ \dot{\psi}_t = v_t \frac{\tan(\delta_t)}{L_t} \\ \dot{v}_t = a_t \end{cases} \quad (2)$$

In these equations δ_t and a_t are the two input of the system. The first is the steering angle of the two front wheels, and directly affects the heading angle dynamic. The latter is the acceleration, and directly affects the speed dynamic. The position of center of gravity x_t and y_t are indirectly affected by the inputs through the other two states. Then the input vector is

$$u_t = \begin{bmatrix} \delta_t \\ a_t \end{bmatrix} \quad (3)$$

In terms of state space representation, the output y of this system model is composed by the vector of the states itself. The only fixed parameter that appears in these equations is the wheelbase L_t , which is the distance between front and rear axles of the tractor.

2.3. Tractor and implement model

In real-world applications, a tractor often operates with an implement attached. For this reason, in this work the option to calculate the trajectory either with a standalone tractor or with a tractor and implement system has been included. A single axle trailer is considered attached to the tractor through a hook, as shown in Figure 5.

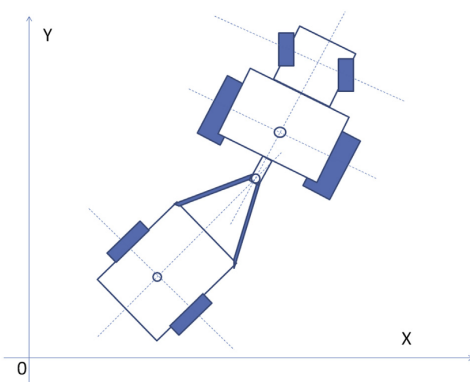


Figure 5: Tractor and implement representation⁴

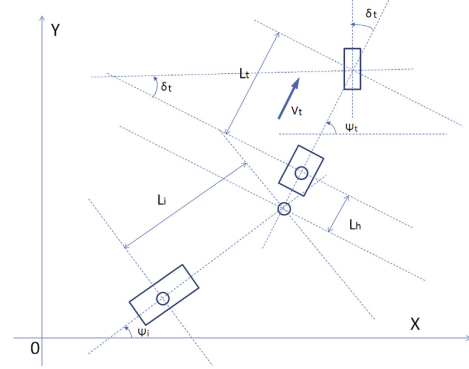


Figure 6: Kinematic bicycle model of tractor and implement⁴

Also in this case, the model used to describe the behavior of the system is a coupled pair of kinematic bicycle models, as the one illustrated in the Figure 6.

It follows that, in addition to the state of the tractor already described, other four states must be added:

⁴Images taken from [3]

- The position of the center of gravity of the implement on the X and Y axis, labeled as x_i and y_i
- The heading angle of the implement, labeled as ψ_i
- The speed of the center of gravity of the implement, labeled as v_i

Thus, a total of 8 states are obtained, represented in the following state vector

$$z = \begin{bmatrix} z_t \\ z_i \end{bmatrix} = \begin{bmatrix} x_t \\ y_t \\ \psi_t \\ v_t \\ x_i \\ y_i \\ \psi_i \\ v_i \end{bmatrix} \quad (4)$$

As already said in the assumptions paragraph (Section 2.1), the length of the hook is considered negligible and omitted in the formulation of the dynamic equation of the states.

Due to the passive attachment of the implement, its states are influenced by the heading and speed of the tractor, and no additional input variables are introduced.

Two auxiliary quantities can be employed to model its behavior.

$$\delta_i = \psi_t - \psi_i \quad (5)$$

$$v_i = v_t \cos(\delta_i) \quad (6)$$

The first is the difference between the headings of the tractor and the implement, and can be seen as a sort of steering angle for the latter. The second variable is the speed of the tractor multiplied by the cosine of difference between the two headings, and represents the longitudinal speed of the implement. Then, the dynamic equations in continuous time describing the evolution of the four implement states are

$$\begin{cases} \dot{x}_i = v_i \cos(\psi_i) \\ \dot{y}_i = v_i \sin(\psi_i) \\ \dot{\psi}_i = v_i \frac{\tan(\delta_i)}{L_i} \\ \dot{v}_i = a_t \cos(\delta_i) - \frac{v_t^2 \sin(\delta_i) \tan(\delta_t)}{L_t} + \frac{v_t^2 \sin(\delta_i)^2}{L_i} \end{cases} \quad (7)$$

In these equations just two fixed parameters appears, that are tractor wheelbase L_t and implement wheelbase L_i .

3. Problem Abstraction

This chapter outlines the methods used to address the following objectives:

- **Minimization of execution time:** In agricultural operations, optimizing working time is crucial, as agricultural businesses aim to maximize the efficiency of their machinery across land and production cycles. Reducing idle time –periods when the machine is not actively performing tasks in the field– is important for enhancing overall productivity.
- **Robustness to Various Headland Configurations:** Agricultural terrains often feature irregular and non-standard field layouts. Therefore, the algorithm must be adaptable to different operational area setups, ensuring reliable performance across varying headland configurations.
- **Selection Among Different Maneuvering Options:** As discussed in Section 4.2, different headland layouts may limit the set of feasible maneuvers. These variations require the proposed solution to consider and select the most appropriate maneuvering option.

3.1. Numerical Integration

To solve an optimization problem, a correct simulation of the system in study is crucial. But since the analytical solution to its dynamic equations cannot be directly computed, numerical integration methods must be used. This implies a discretization of the system dynamics, which introduces approximation errors that can have a significant impact on the final outcome accuracy. Depending on the chosen method and on the discretization step, the simulation could be either very accurate but slow, or faster but leading to a higher simulation error.

To choose the best numerical integration technique to use, four methods have been studied, running simulations and comparing the resulting errors and elapsed time:

- Forward Finite Differences (FFD)
- Second order Runge-Kutta (RK2)
- Third order Runge-Kutta (RK3)
- Fourth order Runge-Kutta (RK4)

To compare them, the Matlab function ODE45 has been used as ground-truth. This is a function that is used for numerical integration that leads to a very accurate result, but in a considerable amount of time. This is why it has been chosen only as ground-truth and not as numerical integration method to use.

When deciding on the numerical integration technique to use, it is important to consider the acceptable error margin. Given the particular application of this optimization problem, a tractor that is maneuvering in a field, the limit of the maximum acceptable error is set to $0.05m$.

The simulations consists of operating the tractor for a period of 10 seconds, running at maximum allowed speed v_{\max} and turning using the maximum allowed steering angle δ_{\max} . This is to simulate the system in the worst possible condition, in order to catch the highest possible error. The result is that the vehicle follows a circular trajectory like the one shown in Figure 7a.

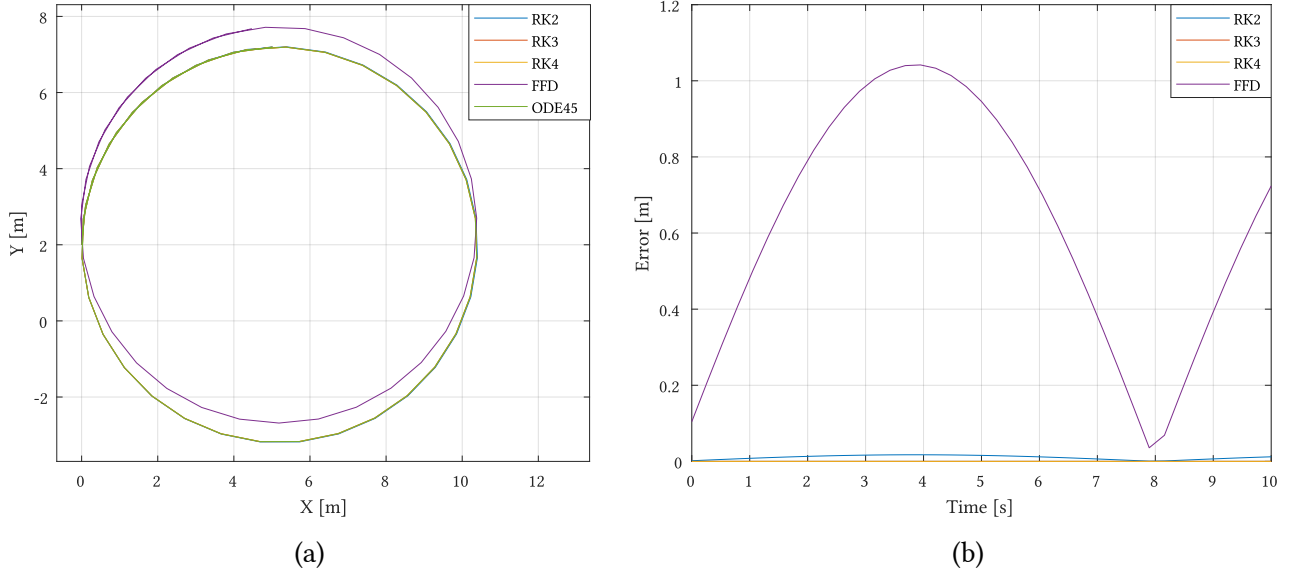


Figure 7: Comparison between trajectories (7a) and errors (7b) generated using different integration methods over time at a sampling time of. $T_s = 0.25 \text{ s}$

This simulation is repeated using the function ODE45 and the others four integration method for a set of six different sampling times (T_s):

$$T_s = [0.01 \text{ s}, 0.025 \text{ s}, 0.05 \text{ s}, 0.1 \text{ s}, 0.25 \text{ s}, 0.5 \text{ s}] \quad (8)$$

The so obtained computational time and maximum error for each method and sampling time are shown in the following tables Table 3a and Table 3b. The error is computed using the distance between each point of the simulation and the corresponding point on the ground-truth trajectory. Figure 7b shows its evolution over time.

To evaluate the accuracy of the methods, the maximum error was selected over the average error because the constraint on allowable error pertains to the maximal tolerance. As illustrated in Figure 7b, the error varies significantly throughout the maneuver, meaning that while the mean error might remain below the set threshold, the maximum error could still exceed it.

Ts [s]	ODE45	RK2	RK3	RK4	FFD
0.01	8.17e-01	1.41e-02	2.51e-02	3.04e-02	8.01e-03
0.025	3.38e-01	8.92e-03	1.85e-02	2.75e-02	5.37e-03
0.05	1.98e-01	3.87e-03	6.23e-03	7.85e-03	2.07e-03
0.1	5.13e-02	1.26e-03	1.88e-03	2.60e-03	7.32e-04
0.25	2.09e-02	5.28e-04	8.24e-04	1.32e-03	3.36e-04
0.5	1.19e-02	2.72e-04	3.67e-04	5.28e-04	1.36e-04

(a) Elapsed time to run simulation [s]

(b) Maximum error with respect to ODE45 [m]

Table 3:

The first observation from Table 3a is that, as previously mentioned, the simulation using the ODE45 function is significantly slower than all other methods. For this reason, ODE45 has not been considered a possible integration method for the simulations.

Moreover, an analysis of the data reveals that while the FFD method is the fastest, it results in a significantly higher error. This is also evident in Figure 7a and Figure 7b, where the other methods are nearly indistinguishable from the ground truth, whereas the FFD method deviates noticeably.

The RK3 and RK4 methods both produce an almost identical and minimal error, approximating to zero. However, given the longer computation time of RK4, RK3 is identified as the more efficient choice between the two.

Given these considerations, the decision of the best numerical integration method falls inevitably between RK2 and RK3. Looking at the Table 3b, it can be noticed that when $T_s \leq 0.25s$ both methods largely satisfy the condition on maximum allowable error. And so, considering a sampling time below that value, the best method to use is RK2, since it finds the solution in a short amount of time and with a more than acceptable simulation error.

3.2. Optimization problem

The control algorithm presented falls into the a category of *Finite Horizon Control Problem (FHOCP)* which is the design of an *input sequence* that minimizes a chosen cost criterion. This is typically expressed in the time domain over a finite horizon, ranging from t (initial time) to $t + N$ (final time), where N is called prediction horizon. Moreover, state and input constraints are also present in general, and shall be satisfied by the designed input sequence.

In this work, the prediction horizon is fixed at N_s time steps. However, since the objective is to minimize the overall execution time, the sampling time T_s is included as a variable. Given that the total time required to complete the maneuver is $N_s \cdot T_s$, minimizing T_s directly reduces the execution time.

Therefore, the complete vector of variables to be optimized is composed by the input sequence of the system U and by the sampling time T_s . In light of these considerations, the mathematical formulation of the problem is given by the Eq. (9).

$$\min_{U, T_s} \quad \gamma \cdot p \cdot |z_f - z(N_s|t)|^T + (1 - \gamma)N_s T_s \quad (9a)$$

$$\text{subjected to} \quad (9b)$$

$$z(i+1|t) = f_z(z(i|t), u(i|t), T_s) \quad i = 0, \dots, N_s - 1 \quad (9c)$$

$$y(i|t) = g_z(z(i|t), u(i|t), T_s) \quad i = 0, \dots, N_s \quad (9d)$$

$$h(z(i|t), u(i|t)) \leq 0 \quad i = 0, \dots, N_s \quad (9e)$$

$$l_b \leq U \leq u_b \quad (9f)$$

$$z(0|t) = z_0 \quad (9g)$$

in which N_s is the simulation horizon, (9c) and (9d) represent the evolution over time of the model already described in Section 2.2 and U is the input sequence of the system that must be optimized by the solver engine, described as below:

$$U = [u(0|t), \dots, u(N_s|t)]^T = \left[\begin{bmatrix} \delta_t(0|t) \\ a_t(0|t) \end{bmatrix}, \dots, \begin{bmatrix} \delta_t(N_s|t) \\ a_t(N_s|t) \end{bmatrix} \right]^T \quad (10)$$

In the following sections, a specific description of the components of the formulated optimization problem are provided. The explanation primarily focuses on the tractor model only, followed by a dedicated section that outlines the differences when the implement is also considered.

3.2.1. Initial and final states

According to maneuver characteristics that has been already introduced and can be seen in Figure 1, the initial and final states are described below, where all variables refers to the tractor only and subscript x_t has been omitted for clarity of notation.

$$z_0 = \begin{bmatrix} x_0 \\ y_0 \\ \psi_0 \\ v_0 \end{bmatrix} \quad z_f = \begin{bmatrix} x_f \\ y_f \\ \psi_f \\ v_f \end{bmatrix} \quad (11)$$

The initial position is $(x_0, y_0) = (0, 0)$ while the final one (x_f, y_f) is determined based on the headland's linear approximation.

$$\begin{cases} x_f = x_0 + d \\ y_f = m_{\text{low}} \cdot x_f + q_{\text{low}} \end{cases} \quad (12)$$

Where $m_{\text{low}}, q_{\text{low}}$ are characteristic parameters of the linear expressions of the headland limits, explained in detail in Section 3.4.2.2. Heading angle corresponds to $\psi_0 = -\psi_f = \frac{\pi}{2}$, while the final and initial velocity are the same, i.e., $v_0 = v_f = 1.11 \text{ m/s}$. The specific differences between this tractor-only model and the tractor-implement model are detailed in the Section 3.5, where the unique considerations for each configuration are thoroughly discussed.

3.3. Cost function

The cost function that has been implemented is

$$\min_{U, T_s} \gamma \cdot p |z_f - z(N_s|t)|^T + (1 - \gamma) N_s T_s \quad (13)$$

It is a multi-objective cost function. Indeed two conflicting terms are included. The first one is the difference between the desired final states z_f and the ones at the end of the horizon $z(N_s|t)$ obtained running the simulation of the system. It represents the accuracy of arrival in the final point. The second is the cost representing the whole execution time. These two objectives are conflicting: achieving a quicker maneuver may compromise accuracy in reaching the final states, potentially resulting in a slightly incorrect heading angle or position. On the other hand, improving accuracy in the final states requires additional time to complete the maneuver.

Moreover a weighting vector p is used to give some states more importance than other in being as close as possible to the desired final ones, according to their unit of measurement. Indeed, since in agricultural application is acceptable to have tolerances in the order of centimeters, is addressable to focus the solver on the orientation ψ_t that is the main feature to ensure the rows to be parallel. In the following table are summarized the elements of the p vector and final state error tolerances (which are well described in Sec. 3.4.2.3). Both vectors pertain to the states of the tractor and of the implement.

	x	y	ψ	v
p	1	1	5	1
tol_f	0.05	0.05	$\frac{5\pi}{180}$	3.6
unit	m	m	rad	m/s

Table 4: Table of weight vector with respect relative tolerances

3.3.1. Multi-objective approach

In literature there are three strategies to approach multi-objective problems:

1. Including all objectives except one as constraints, for example by setting maximum values that they shall not be exceeded, and optimizing the remaining one
2. Introducing a vector of positive scalars to multiply the cost terms and optimizing the weighted sum of them
3. A mix of 1. and 2.

In this case study the third method has been used. Indeed the maximum allowed error on the final states is enforced using the constraints, and setting it lower or equal to some predefined tolerances tol_f , whose values are reported in Table 4. This is better explained in the Section 3.4. Moreover, a positive scalar γ varying from 0 to 1, is used to weight the two costs. In particular on the first term the weight is given directly by γ , while on the second one it is given by $1 - \gamma$. In this way by setting its value to 0 the focus is entirely on speed, whereas when it is equal to 1 only the accuracy on final state error is considered.

In this project $\gamma = 0.15$ is used. This value has been chosen because, since the constraints ensure that the maximum error at the target point is below a certain threshold, more emphasis is given to the time required to complete the maneuver. However, it is not equal to zero since otherwise the final states would always lay on the limit of the tolerances. In this way the final accuracy can be still improved, where possible.

3.4. Constraints

To meet the objectives of this work, both linear and non-linear constraints were implemented. The linear constraints address input saturation limits, while the non-linear ones define the boundaries of the headland's prohibited area and capture the dynamics of the model. In particular, (9c) and (9d) refer to the dynamical evolution of the system, computed with Runge-Kutta 2-th order method imposing z_0 as initial condition (9g).

3.4.1. Linear Inequality constraints

The linear inequality constraints are intended to keep the input variables inside actuator limits and to ensure that the assumptions made in Section 2.1 are valid. In particular a threshold was set on the maximum and minimum value of these variables for each considered time instant, and so all of this conditions are merged into only two vectors according to dimension of the vector U .

$$\begin{aligned} \delta_{\min} \leq \delta_t \leq \delta_{\max} & \quad \rightarrow \quad l_b \leq U \leq u_b \\ a_{\min} \leq a_t \leq a_{\max} \end{aligned} \tag{14}$$

3.4.2. Non linear Inequality constraints

Even if the expression of the following constraint is linear, it is important to remark that the non-linearity lays in the fact that variables involved, such as X, Y position, velocity v_t , and states vector z_t , depends on the optimization variable U through the numerical integration of the model (Equations 9c and 9d), that involves high non-linearities. In the following paragraphs each elements of Eq. (15) are described in details, referring to the only tractor case.

$$h = \begin{bmatrix} -V_t - c_{\text{vel}} \cdot v_{\max} \cdot \mathbb{I}_{1 \times N_s} \\ +V_t - v_{\max} \cdot \mathbb{I}_{1 \times N_s} \\ Y_t - m_{\text{up}} \cdot X_t - q_{\text{up}} \cdot \mathbb{I}_{1 \times N_s} \\ -Y_t + m_{\text{low}} \cdot X_t + q_{\text{low}} \cdot \mathbb{I}_{1 \times N_s} \\ |z_t(N_s) - z_f| - \text{tol}_f \end{bmatrix} \tag{15}$$

Where $\mathbb{I}_{1 \times N_s}$ is a vector of ones of dimension $1 \times N_s$ and the following notation is been used.

$$V_t = [v_t(0|t), \dots, v_t(N_s|t)]^T \quad X_t = [x_t(0|t), \dots, x_t(N_s|t)]^T \quad Y_t = [y_t(0|t), \dots, y_t(N_s|t)]^T$$

3.4.2.1. Velocity saturation

To satisfy assumptions on the slow velocity and limits on the motor the following upper and lower bounds are included and disposed below in a summarized way.

$$-v_{\max} \cdot c_{\text{vel}} \cdot \mathbb{I}_{1 \times N_s} \leq V_t \leq v_{\max} \cdot \mathbb{I}_{1 \times N_s} \quad (16)$$

It's important to remark the usage of the parameter $c_{\text{vel}} \in \{0, 1\}$. This allows to force the tractor to proceed only forward when $c_{\text{vel}} = 0$, while $c_{\text{vel}} = 1$ it makes the tractor to exploit the reverse gear. The motivation is well described in Section 4.2.

3.4.2.2. Headland Area constraints

Main objective of the algorithm consists in maintaining the tractor inside the operational area delimited by the headland limits. Linear approximation has been used to represent them, as can been seen in the figure Figure 2.

$$Y_t \leq m_{\text{up}} \cdot X_t + q_{\text{up}} \cdot \mathbb{I}_{1 \times N_s} \quad (17a)$$

$$Y_t \geq m_{\text{low}} \cdot X_t + q_{\text{low}} \cdot \mathbb{I}_{1 \times N_s} \quad (17b)$$

Coefficients m_{up} , m_{low} and q_{up} , q_{low} are the slope and the constant terms of the upper and lower boundaries respectively.

3.4.2.3. Final states tolerances

The ideal solution would be to have an equality constraint on the final state request. This in practice is not a strictly requirement for the application and from a solver point of view, since this type of constraints slows down the optimization routine. For these reason an inequality constraint in the following form has been introduced.

$$|z_t(N_s) - z_f| \leq tol_f \quad (18)$$

where tol_f is a vector in which are specified the tolerances for the final state with respect to the desired one. The values contained in the tolerance vector are contained in Table 4. Eq. (18) represents the maximal values of the error term, constrained according to the multi-objective approach described in Section 3.3.1.

3.5. Tractor and implement variations

When the selected model is the coupled system tractor and implement, some constraints of Eq. (15) need to be modified. As already discussed in Section 2.1, the tractor itself may enter the prohibited area of the field before reaching the final position, while the trailer must remain inside the delimited area, but both of them can't go beyond the upper headland limit. The constraints are then modified as follows.

$$Y_t \leq m_{\text{up}} \cdot X_t + q_{\text{up}} \cdot \mathbb{I}_{1 \times N_s} \quad (19a)$$

$$Y_i \leq m_{\text{up}} \cdot X_i + q_{\text{up}} \cdot \mathbb{I}_{1 \times N_s} \quad (19b)$$

$$Y_i \geq m_{\text{low}} \cdot X_i + q_{\text{low}} \cdot \mathbb{I}_{1 \times N_s} \quad (19c)$$

Where the same notation previously introduced has been used, with according subscripts.

It follows that also initial and final condition need to be modified consistently, in particular some considerations need to be done. In fact, in this case the maneuver starts when the trailer has just exited the field, and the tractor is already in the headland, and ends when the tractor is inside the field. So, for the implement the same starting and terminal conditions of the previous case are used, whereas those for the tractor must be adjusted according to the model. Specifically, the equations in Eq. (20) show how the tractor's x and y positions are set. They are valid either for initial and final positions, so for the sake of clarity subscripts x_0 or x_f are omitted.

$$\begin{cases} x_t = x_i + L_i \cos(\psi_i) \\ y_t = y_i + L_i \sin(\psi_i) \end{cases} \quad (20)$$

Since the rows must be aligned and traveled at constant speed, the initial and final heading error and velocity are equal for both tractor and implement. In particular their value are the same of the tractor-only case, reported in Section 3.2.1.

Moreover, the relative angle between the two headings must be controlled, due to the fact that the two vehicles can't physically overlap and tow has angle limits. To this scope the Eq. (21) has been included in the constraints vector.

$$|\psi_t - \psi_i| - \delta_{i_{\max}} \leq 0 \quad (21)$$

Regarding the final state tolerance, the vector of maximum allowed error tol_f needs to be extended, increasing from four states to eight. Its values are the same as in the tractor-only case, but are repeated for the four states of the implement as well. The form of the constraint equation is the same as before, and is represented in Eq. (18).

4. Optimization procedure

In this chapter, the optimization problem is approached from a practical perspective. Specifically, adjustments were made to improve solver performance, taking into account the system characteristics identified during the implementation phase.

4.1. Downsampling input variables

In an optimization problem the time needed to find the solution is highly affected by the number of optimization variables. In this work, the optimization variables are the vectors of input of the system, that are steering angle δ_t and acceleration a_t , and the sampling time T_s .

A possible approach to speed up the resolution of the problem, is by downsampling the input variables of the system. Instead of computing the input values at every simulation step, they are calculated at intervals, using the last computed value to control the system until the next computation. This significantly reduces the number of optimization variables, speeding up the process of finding a solution. In particular, in this work, it was decided to compute the value of the input variables each 2 time steps.

4.2. Possible maneuvers

As it also described in [3], to perform a turn in a field from one row to the next, there are two possible types of maneuver: the bulb turn and the fish tail turn.

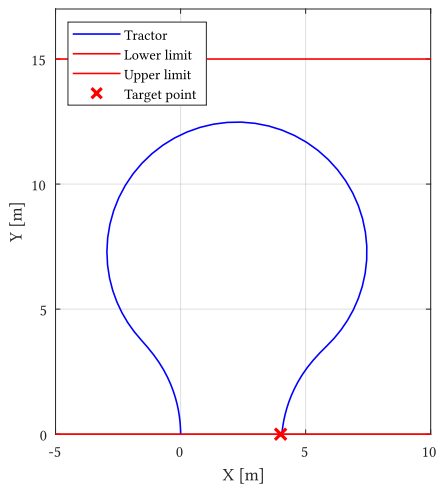


Figure 8: Bulb trajectory

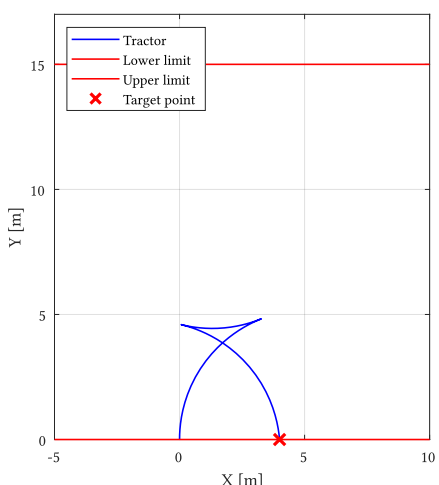


Figure 9: Fish tail trajectory

The first one, represented in Figure 8, is performed with positive speed only. It is called in this way since its shape reminds of a bulb light.

At the beginning of the maneuver, the tractor initially steers away from the target point to create space for the turn, then moves closer by reversing the steering angle, and finally adjusts the steering again to align with the desired final angle and reach the endpoint. This trajectory is characterized by high speed of travel, but big covered distance. Unfortunately it requires the width of the headland to be very high, because a lot of space is needed to perform the maneuver.

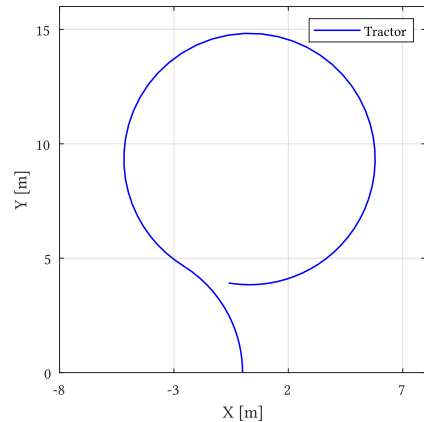
The second option is represented by the fishtail trajectory, like the one shown in Figure 9. In contrast to the bulb trajectory, this approach allows for negative speeds. Initially, the tractor steers directly toward the endpoint, then executes a reverse maneuver before moving forward again to reach the final target point.

This kind of maneuver contrasts with the previous one, since it is characterized by low speed of travel and low covered distance, with a lower exploitation of the headland with respect to the previous one.

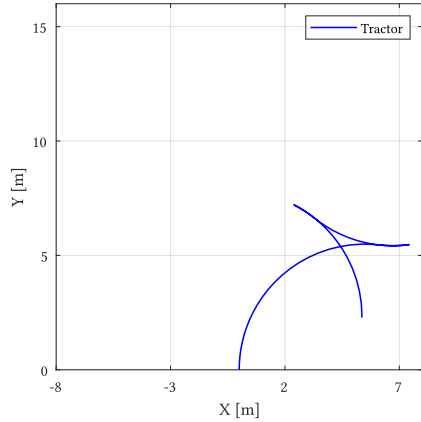
4.3. Initial condition

In an optimization problem, a key role is played by the initial conditions. In fact, since this is an highly non linear problem, the cost function could have lots of local minima. Hence, according to the initial condition chosen, different solutions might be discovered. Moreover also the time needed to complete the optimization is affected, since if the starting point is close to the final result, the search process is faster.

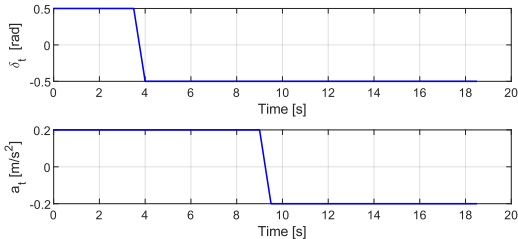
As previously explained, two possible maneuvers are considered: the bulb and fishtail trajectories. Knowledge of these desired solutions can be incorporated into the initial conditions, providing two input sequences U_0 starting from the initial states z_0 . This approach generates two trajectories that closely approximate the expected final outcome, as shown in the following graphs.



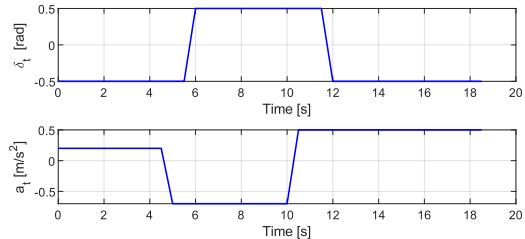
(a) Initial trajectory for bulb



(b) Initial trajectory for fishtail



(c) Starting input sequence for bulb



(d) Starting input sequence for fishtail

As can be noticed in the Figure 10a and Figure 10c, some of the typical characteristic of the bulb trajectory are contained in the initial condition used to find it, such as only positive speed and the initial turn away from the target point. Additionally, the acceleration profile shares some similarities with the desired final result, as the initial input provided to the solver features positive accelerations during the first half of the simulation steps and negative accelerations in the latter half.

Similar considerations can be done looking at the Figure 10b and Figure 10d. Indeed, in this case, the similarities with the final trajectory include the presence of a segment in reverse gear and the change of steering direction within that section. To achieve this, after a brief phase of acceleration, a negative input is applied to reduce speed and move backward. During this segment, also the turning direction changes. Then the speed is increased again and the steering angle reversed, to reach the target point.

In both of the two possible initial conditions, the starting value of the sampling time is set to $T_s = 0.25s$. This choice is done since, as explained before, for values of sampling time equal or lower than

this threshold, the choice of RK2 as numerical integration method is justified and leads to low simulation errors.

4.4. Implemented optimization problem

An interesting aspect that has to be highlighted is that, even if it has a higher distance to travel, the tractor reaches the target point in lower time when performing the bulb trajectory. This is due to the much higher speed that can be reached when executing it.

In this work the considered objectives are to complete the maneuver in the lower possible time, but maintaining the possibility to find a solution in different headland conditions. Considering this, the bulb trajectory would be the preferred option, since it is faster. But unfortunately, if the width of the headland is too low, it is not feasible and the fishtail trajectory is the only option.

The developed approach, consists in the possibility to solve two subsequent optimizations. In the first one, a solution is searched using the bulb turn. This is done giving proper initial condition and setting the value of the variables $c_{\text{vel}} = 0$ to force the tractor to move only forward. If a feasible trajectory is found, in light of the previous statements, it is known a priori that it is the fastest possible, and is kept as final solution. Then the value of constraints violation is checked. If lower than a threshold, set to $1e - 6$, it is considered a viable solution. Otherwise, a second optimization is performed using the fishtail initialization and $c_{\text{vel}} = 1$ to allow also the negative speed. Then the constraint tolerance is checked again. If it is violated, none of the two maneuver can reach the target point satisfying the constraints, and an error message is displayed.

To explain this concept in a better way, a pseudo algorithm is represented below

```

1: function MAIN()
2:   ▷ Initialize optimization variable for bulb trajectory
3:    $c_{\text{vel}} \leftarrow 0$ 
4:
5:   ▷  $[\text{exitflag}, \dots] = \text{fmincon} (\dots)$ 
6:   if  $\text{exitflag.constr\_violation} > \text{constr\_tol}$  then
7:      $c_{\text{vel}} \leftarrow 1$ 
8:     ▷  $[\text{exitflag}, \dots] = \text{fmincon} (\dots)$ 
9:
10:    if  $\text{exitflag.constr\_violation} > \text{constr\_tol}$  then
11:      ▷ No valid solution found
12:      return error message

```

4.5. Optimization tools

To solve the optimization problem, the Matlab© environment was used, specifically the `fmincon` function. This tool is designed to handle constrained nonlinear optimization problems. `Fmincon` was chosen because it finds solutions quickly, especially when complex constraints and nonlinearities are involved.

Another major benefit of `fmincon` is how customizable it is. The solver allows to adjust many internal settings that control how the optimization is done, visualize the evolution of the system during the optimization routine, and stopping conditions. Some of these settings were left at their default values, but others were modified to improve the solver's performance for this specific problem.

In particular the setted values are:

- **Algorithm = interior-point** → The interior-point method is known for handling constraints effectively and is particularly well-suited for large-scale optimization problems.
- **MaxIterations = 250** → This limits how long the optimization process can continue before stopping, even if no optimal solution is found.
- **MaxFunctionEvaluations = 1e6** → Function evaluations refer to how often the objective function is computed, and limiting this ensures that the optimization process remains computationally feasible.
- **HessianApproximation = bfgs** → Determines the method used by the solver to approximate the Hessian matrix of the objective function. The BFGS method (Broyden–Fletcher–Goldfarb–Shanno) is a quasi-Newton method, offering a good balance between computational efficiency and accuracy in estimating the curvature of the cost function.
- **FiniteDifferenceType = central** → The central difference is more computationally demanding than forward or backward difference methods, but it is more accurate compared to them. So the larger computational cost may be compensated by a lower number of iterations in the optimization routine.
- **StepTolerance = 1e-8** → : This ensures the algorithm stops when the step size of the optimization variables variation becomes sufficiently small, indicating convergence towards an optimal solution.
- **OptimalityTolerance = 10e-10** → Sets the termination tolerance for the first-order optimality condition. The solver stops when the gradient of the objective function is small enough, suggesting that a local minimum has been reached.
- **Display = iter** → Configures the solver to display output at each iteration, providing insights into the optimization process.
- **PlotFcn = plotfun_tractor_states** → Instructs the solver to use a custom function, `plotfun_tractor_states`, to plot the trajectory and the values of the optimization variables during the iterations, giving a visual representation of how the solution evolves.

5. Results

The resolution of the optimization problem, solved as explained in the previous chapters, gives very good results. Indeed it can find the optimal trajectory in every configuration of the headland, in a relatively short amount of time, considering only the tractor or the tractor and implement. In the following sections the results obtained in different configurations are presented. In every case, the parameters of the linear approximation of the upper limit of the operational area are reported, i.e., the angular coefficient m and the constant term q ($y = m \cdot x + q$).

5.1. Tractor only

5.1.1. Horizontal wide headland

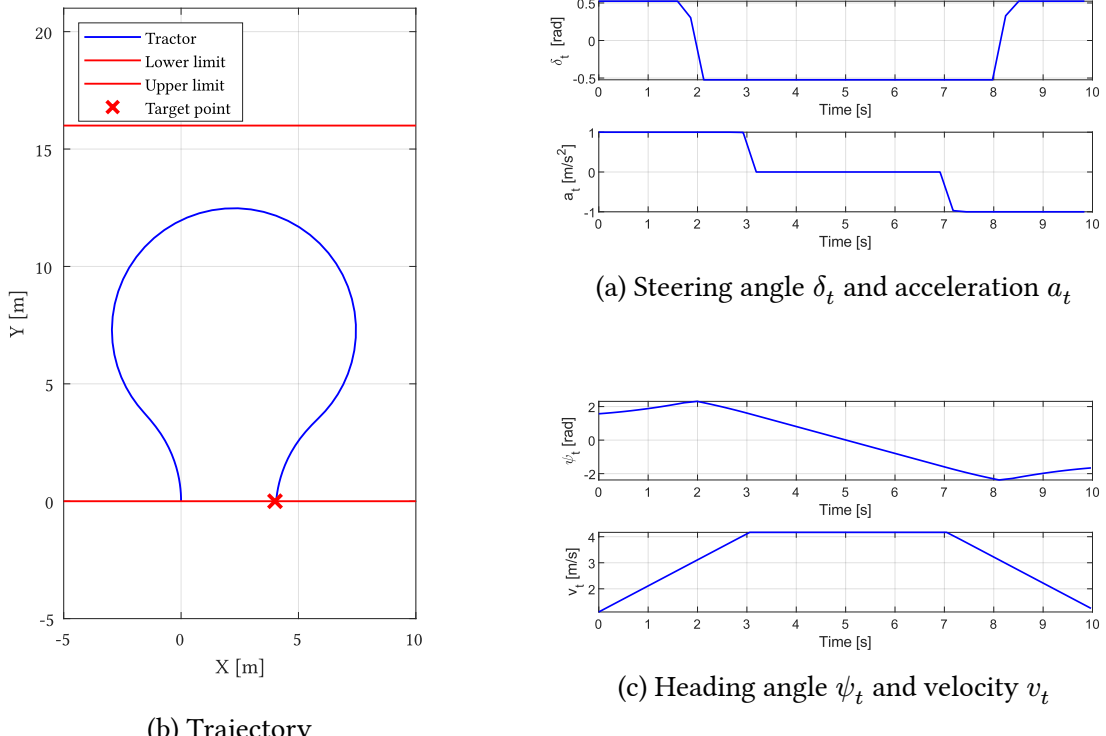


Figure 11: Graphical results of the optimization problem considering only the tractor, and $m = 0$ and $q = 16$ to approximate the upper limit of the headland

Focusing on the solution found for horizontal wide headland traveled with the tractor only, the vehicle reaches the target point performing a perfect bulb trajectory, as can be seen from the image Figure 11. In fact, it is almost perfectly symmetrical, starting with a leftward turn to widen the curve, followed by a large rightward arc, and finally another leftward adjustment to reach the target point with the desired values of the states.

Another very important aspect that can be observed looking at the optimization results is the behavior of steering angle and acceleration, which are well illustrated in the Figure 11. Looking at the steering angle, as previously noted, it initially reaches the maximum left turn, then shifts to maximum right, and finally returns to the full left at the end. Regarding the acceleration, the maximum value is applied at the beginning. In this way the speed saturation limit is quickly reached, and so zero acceleration must be applied for the central part of the maneuver. In the final section the maximum possible deceleration must be used to reached the desired final speed. It is immediately evident that both have very sharp

transitions over time, and both reaches the saturation limits. This particular behavior of the control variables suggests that the found solution is the optimal one.

The fact that in this trajectory the maneuver is performed using the maximum possible speed, can also be clearly observed in the speed graph over time in Figure 11, where, as consequence of the acceleration input, it rapidly reaches the limit value, and at the end drops down until the desired final speed

Optimization results			
Opt. runtime [s]	32.127	T_{end} [s]	9.969
T_s [s]	0.132		

Final states error			
error X_t [m]	0.049	error Y_t [m]	$5.958 \cdot 10^{-11}$
error ψ_t [rad]	0.087	error v_t [m/s]	0.138

Table 5: Numerical results of the optimization problem considering only the tractor, and $m = 0$ and $q = 16$ to approximate the upper limit of the headland

Looking at the final error summarized in Table 5 it can be noticed that none of the final states exceed the threshold values, and, where possible, it is also decreased. This happens because the value of gamma is set to $\gamma = 0.15$, which places greater emphasis on minimizing the time required to complete the turn. As a result, most of the final state values tend to be close to the threshold limits, especially the speed, that must be increased as much as possible to decrease the execution time. However, some importance is still assigned to accuracy, allowing the error in the y-coordinate to be reduced.

Concerning the sampling time, that is the last considered optimization variable, its final value is $T_s = 0.132$ s. This means that during the optimization it has been reduced, since the starting value was 0.25 s. Moreover, that value was the threshold set as hypothesis the use of RK2 as numerical integration method, and so its use is justified.

The final aspect to consider in the optimization results is the time required to find the solution. In this particular case, where only the bulb trajectory must be found, just one optimization must be performed. This means that the time needed is low, and close 30 seconds.

5.1.2. Tilted wide headland

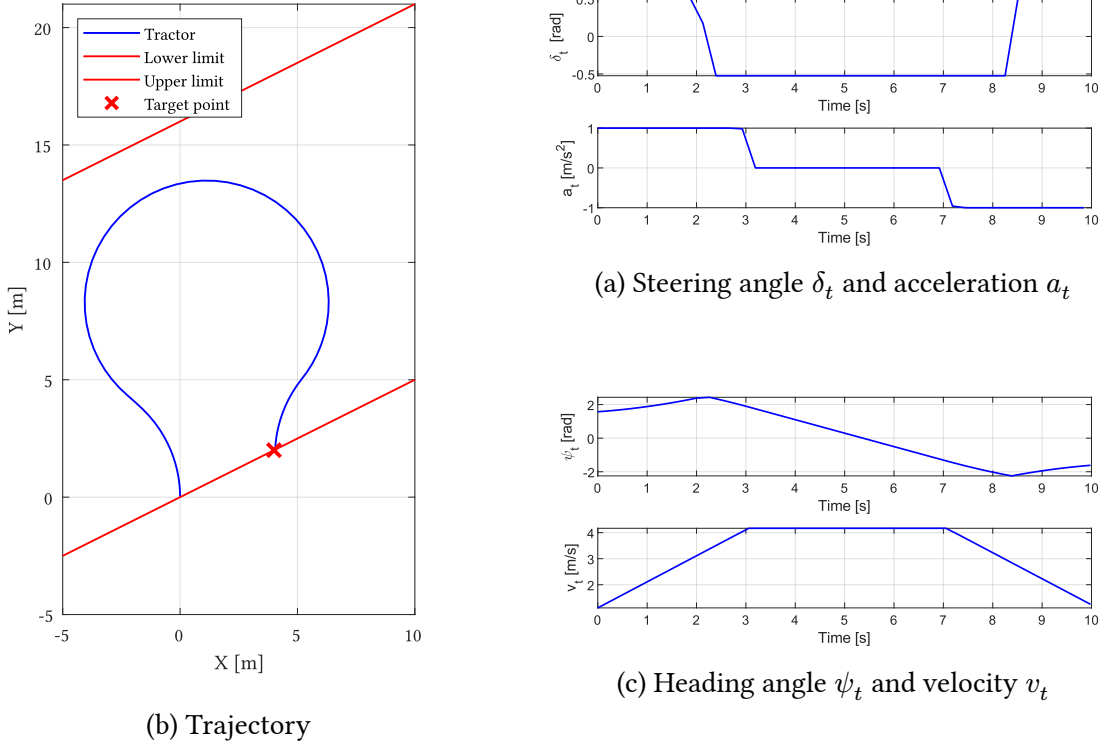


Figure 12: Graphical results of the optimization problem considering only the tractor, and $m = 0.5$ and $q = 16$ to approximate the upper limit of the headland

If instead of horizontal, the headland limits are tilted with respect to the initial tractor heading angle, the result is like the one shown in Figure 12. The considerations that can be done in this situation, are similar to the previous case, except some particular aspects.

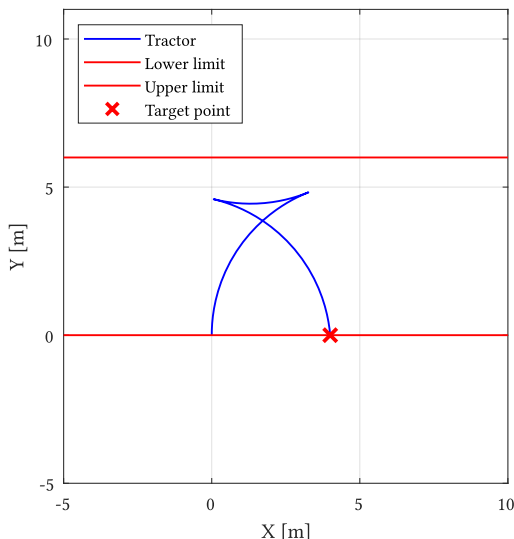
The first is that the trajectory is not symmetric since the initial left turn is wider than the final one. This is also evident from the steering angle graph, which clearly shows that the initial turn lasts longer than the final one. This asymmetry occurs because, with tilted boundaries, the target point is positioned higher than the starting point.

Optimization results			
Opt. runtime [s]	23.278	T_{end} [s]	9.979
T_s [s]	0.133		
Final states error			
error X_t [m]	0.049	error Y_t [m]	0.025
error ψ_t [rad]	0.046	error v_t [m/s]	0.138

Table 6: Numerical results of the optimization problem considering only the tractor, and $m = 0.5$ and $q = 16$ to approximate the upper limit of the headland

Moreover looking at the error of the final point shown in Table 6, it is also clearer what explained before on the reason why some weight is given also to the accuracy, and not only to the time to execute the maneuver. Indeed, in this case only the speed and x error are very close to the tolerated limit. The other states have much lower errors, especially the heading angle, which was high in the previous case. Indeed now its value is 0.046 rad, that corresponds to 2.63 degrees.

5.1.3. Horizontal narrow headland



(b) Trajectory

Figure 13: Graphical results of the optimization problem considering only the tractor, and $m = 0$ and $q = 6$ to approximate the upper limit of the headland

When the problem is solved for a narrow headland, the bulb trajectory is no more feasible, and the only possibility is to perform a fishtail turn. Indeed, as can be seen from Figure 13, it requires less than 5 meters and so it is a viable option.

As already discussed, the particularity of this maneuver is the presence of a reverse section. It is clearly visible in the Figure 13, where the speed assumes negative values in the central part. This is the reason why the speed of travel is much lower than the bulb case, and why it takes more time to perform this trajectory. This behavior is the consequence of the acceleration input over time. Indeed, after an initial increase of speed, a strong deceleration is performed to slow down and move in reverse. Then another strong acceleration is used to restart to move forward and reach the target point.

Optimization results

Opt. runtime [s]	85.664	T_{end} [s]	11.870
T_s [s]	0.158		

Final states error

error X_t [m]	$2.675 \cdot 10^{-6}$	error Y_t [m]	$7.055 \cdot 10^{-5}$
error ψ_t [rad]	0.087	error v_t [m/s]	0.138

Table 7: Numerical results of the optimization problem considering only the tractor, and $m = 0$ and $q = 6$ to approximate the upper limit of the headland

Some important considerations can be done looking at the Table 7. The first regards the sampling time, whose value is $T_s = 0.158s$, that is higher than in the bulb trajectory case. The consequence of this is that also the total execution time is higher. This remarks the difference between the two maneuvering

options, addressed in Section 4.4, that justify the double optimization. Even if the value of the sampling time is higher than before, it is still lower than the limit value set to $T_s = 0.25s$, and so it is justified the use of RK2 as integration method.

Another interesting aspect that can be noticed is that the optimization runtime is quite high compared to the previous cases. This is because some time is lost in the search of a solution using the bulb turn. Only when this is completed and it is checked that it is not feasible, the fishtail trajectory is optimized.

5.1.4. Tilted narrow headland

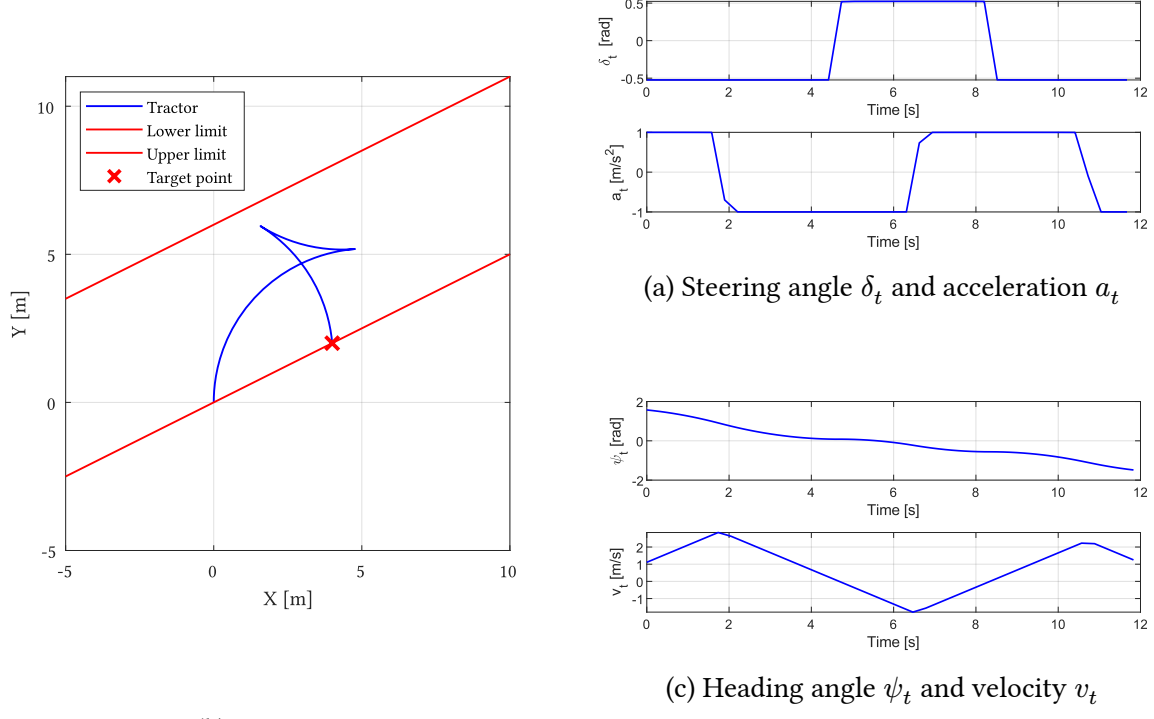


Figure 14: Graphical results of the optimization problem considering only the tractor, and $m = 0.5$ and $q = 6$ to approximate the upper limit of the headland

Considerations similar to the previous case can be done with the tilted condition. The only thing that changes is the fact that it is not symmetric. Indeed looking at the Figure 14, it can be noticed that, like in the case of tilted wide headland, the initial turn lasts longer, because the target point is placed higher than the starting one. This can be seen both in the trajectory graph and in the one of the behavior of the steering angle.

Optimization results			
Opt. runtime [s]	90.854	T_{end} [s]	11.829
T_s [s]	0.157		
Final states error			
error X_t [m]	$6.893 \cdot 10^{-6}$	error Y_t [m]	0.000
error ψ_t [rad]	0.087	error v_t [m/s]	0.138

Table 8: Numerical results of the optimization problem considering only the tractor, and $m = 0.5$ and $q = 6$ to approximate the upper limit of the headland

5.2. Tractor and implement

When both the tractor and its implement are taken in account in the optimization, the observations that can be done on the results are very similar to those made when only the tractor is considered. For this reason, only the results of two cases are presented in the following sections: the tilted wide headland and the tilted narrow headland. This choice was made because these two cases are representative of all the others and include all noteworthy observations. Moreover, only these observations are reported, while considerations similar to the tractor-only case are not repeated.

5.2.1. Tilted wide headland

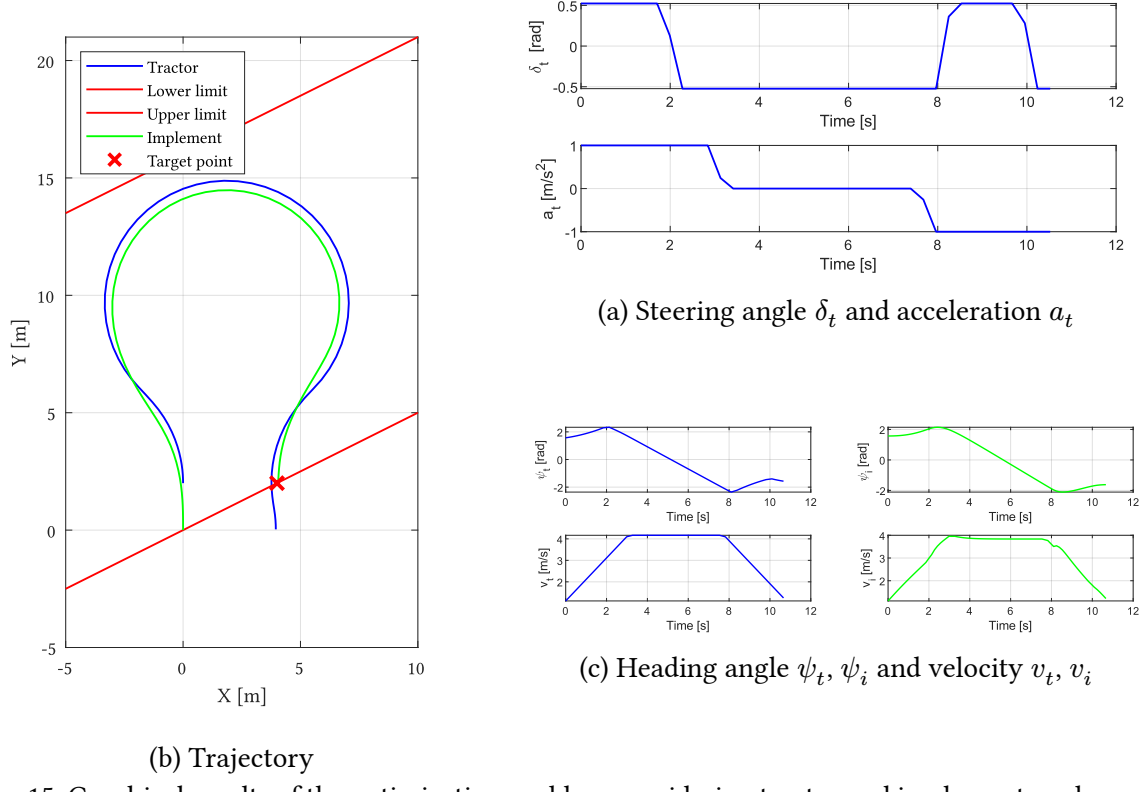


Figure 15: Graphical results of the optimization problem considering tractor and implement, and $m = 0.5$ and $q = 16$ to approximate the upper limit of the headland

The first noticeable difference compared to the previous cases can be observed in the steering angle graph, particularly in the Figure 15. A distinct final change in the steering angle appears, which was absent before. This adjustment is typical in maneuvers that consider the implement and is necessary to realign the tractor with the desired final heading angle and ensure it reaches the target position.

Optimization results

Opt. runtime [s]	23.909	$T_{\text{end}} [\text{s}]$	10.664
$T_s [\text{s}]$	0.142		

Final states error

error $X_t [\text{m}]$	0.049	error $Y_t [\text{m}]$	0.032
error $\psi_t [\text{rad}]$	$9.892 \cdot 10^{-5}$	error $v_t [\text{m/s}]$	0.138
error $X_i [\text{m}]$	0.049	error $Y_i [\text{m}]$	0.025
error $\psi_i [\text{rad}]$	0.050	error $v_i [\text{m/s}]$	0.106

Table 9: Numerical results of the optimization problem considering tractor and implement, and $m = 0.5$ and $q = 16$ to approximate the upper limit of the headland

Another important aspect that changes when also the implement is considered, is that a new constraint must be added. This regards the relative angle between the heading of the tractor and the implement. Its value is well shown in the Figure 16, where also the maximum error allowed is represented. In this particular case, where the the bulb turn is performed, the relative angle is always very low with respect to the threshold. It can be noticed that in two points its value rapidly decreases and became close to 0. This happens in correspondence of the two changes in steering angle, where the heading of the two vehicles realigns for an instant.

In this particular case, where the bulb turn is performed, the relative angle remains consistently low compared to the threshold. Moreover, at two specific points, its value rapidly decreases and approaches zero. This occurs during the two changes in steering angle, where the heading of both vehicles rapidly realigns.

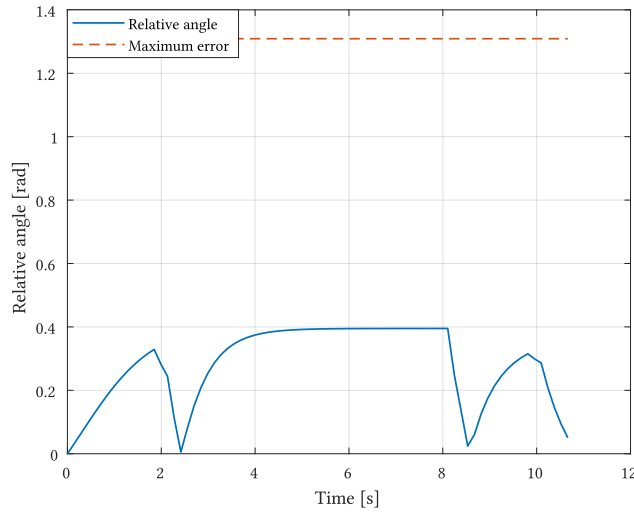


Figure 16: Relative error between heading angle of tractor and implement

5.2.2. Tilted narrow headland

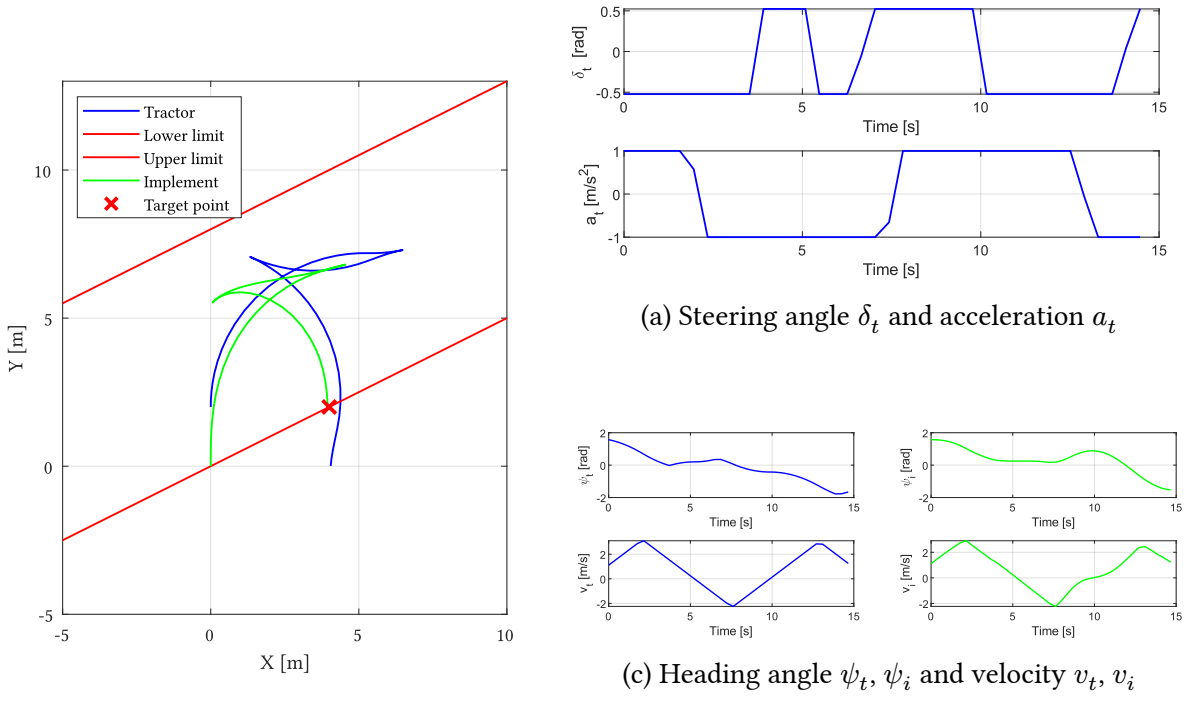


Figure 17: Graphical results of the optimization problem considering tractor and implement, and $m = 0.5$ and $q = 8$ to approximate the upper limit of the headland

The tilted narrow headland is the most difficult considered scenario. Indeed in it the complexity is increased a lot by the reverse section that must be performed with the implement. Looking at the behavior of the acceleration shown in Figure 17, it can be noticed that it is quite similar to the tractor-only case. The big difference in the input variables is given by the steering angle, since its direction is changed more times than previous cases. Indeed, before starting the reverse section, the tractor makes a slight curve to the left. Then, at the beginning of the reverse, it turns to the right before changing the steering angle again and continuing in a manner similar to the tractor-only case. This behavior can also be clearly observed by looking at the trajectory shown in the same image. The reason why this is done is to meet the constraint on the maximum relative angle between the two vehicles, which otherwise would be exceeded.

Optimization results			
Opt. runtime [s]	140.941	T_{end} [s]	14.662
T_s [s]	0.195		

Final states error					
error X_t [m]	0.049	error Y_t [m]	0.008		
error ψ_t [rad]	0.087	error v_t [m/s]	0.138		
error X_i [m]	0.049	error Y_i [m]	$1.607 \cdot 10^{-6}$		
error ψ_i [rad]	0.049	error v_i [m/s]	0.107		

Table 10: Numerical results of the optimization problem considering tractor and implement, and $m = 0.5$ and $q = 8$ to approximate the upper limit of the headland

The behavior over time of the relative angle just described, is shown in the Figure 18. In the graph, it is clearly visible that towards the end of the reverse section, its value increases significantly and reaches the threshold, but never exceeds it.

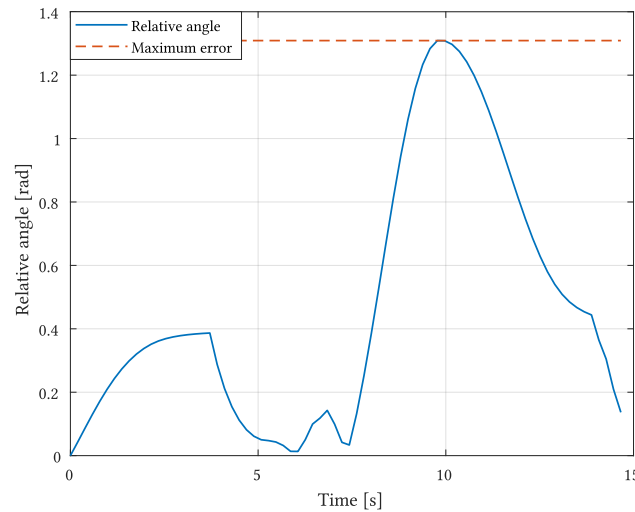


Figure 18: relative error between heading angle of tractor and implement.

6. Conclusions

From the results just presented, it is clear that the established objectives have been fully achieved. The developed algorithm is capable of leveraging the advantages of both types of maneuvers, favoring the bulb turn because it takes less time, but allowing the option to use the fishtail trajectory when the former is not feasible due to the low width of the available space. As consequence of this, various limit configurations of the headland can be handled, and the maneuver to execute is found easily. Moreover in every case the solution is the one that takes the least possible time, making full use of the allowed acceleration and steering angle, while still keeping the final state errors within the threshold values, and so guarantying a good accuracy.

As explained in the introduction, the primary goal of this program is to calculate the optimal trajectory for a tractor, which can then be used as a reference for autonomous or steering-assisted vehicles, in order to optimize working time and, consequently, agricultural production.

Unfortunately, it present some limitations that currently prevent it from being used in practice, mainly connected to the assumptions that has been done. The first is the fact that using the kinematic bicycle model, some dynamical aspects of the behavior of the tractor are neglected, like the force of interaction between tire and soil. It follows that only scenarios with slow and slowly changing speeds can be accounted.

Moreover, in this work a preliminary assumption was done on the limit of the headland, saying that they already account for the physical dimensions of both the tractor and the implement, and thus only their center of gravity (COG) needs to be considered. In real world these dimensions must be taken into account in the trajectory planning phase.

These limitations could be the subject of potential future improvements and implementations. For example, a dynamical model can be used to increase the accuracy of the solution that is found. This would introduce high complexity in the model, but would also significantly enhance the accuracy of the vehicle's behavior description.

Another improvement that could be done, would be to consider in the computations also the dimension of the two vehicles. This is quite a complex task, as it requires considering both their width and length, along with the position of the center of gravity (COG) and the heading angle, to determine their occupancy and assess whether they exceed the headland limits.

The last improvement that could be done is not connected with the assumptions, but with the way the solution is found. Indeed in this project if the bulb turn is not feasible, a double optimization is performed to obtain a fishtail trajectory. This results in a significant loss of time in solving the optimization problem, as most of it is spent trying to solve an unfeasible problem. So, a possible future implementation could be to find a way to skip the first optimization and perform only the second one, in cases where it is known in advance that the first cannot yield an acceptable solution. This could be done performing a gridding on m and q values to determine whether the bulb turn is feasible or not. But it is a very complex task to accomplish. Moreover those threshold values are highly dependent from the parameters of the tractor and its saturation limits, like the wheelbase and the maximum steering angle. Indeed, if the vehicle can turn in a lower amount of space, also the minimum upper limit that allow to perform a bulb turn is lowered.

Bibliography

- [1] “Farmers and the agricultural labour force - statistics.” Nov. 2022. [Online]. Available: https://ec.europa.eu/eurostat/statistics-explained/index.php?title=Farmers_and_the_agricultural_labour_force_-_statistics#Fewer_farms.2C_fewer_farmers
- [2] U.S. Department of Agriculture, “Farm Labor.” Aug. 2023. [Online]. Available: <https://www.ers.usda.gov/topics/farm-economy/farm-labor/#recent>
- [3] Xuyong Tu and Lie Tang, “Headland turning optimisation for agricultural vehicles and those with towed implements.” Dec. 25, 2019. [Online]. Available: <https://www.sciencedirect.com/science/article/pii/S2666154319300092>
- [4] L.M. Fagiano., *Constrained Numerical Optimization for Estimation and Control, Lecture Notes*. 2022.